Journal of Mining and Environment (JME)

journal homepage: www.jme.shahroodut.ac.ir

Shahrood University of Technology

Iranian Society of Mining Engineering (IRSME)

THOMSON REUTERS

Vol. 10, No. 3, 2019, 777-785.

DOI: 10.22044/jme.2019.8285.1708

Processing a multifold ground penetration radar data using common-diffraction-surface stack method

H. Shahsavani

Department of Mining, Faculty of Engineering, University of Kurdistan, Sanandaj, Iran

Received 11 April 2019; received in revised form 24 June 2019; accepted 24 June 2019

Keywords

Ground Penetration Radar

CRS

CDS

Abstract

Recently, the non-destructive methods have become of interest to the scientists in various fields. One of these method is Ground Penetration Radar (GPR), which can provide a valuable information from underground structures in a friendly environment and cost-effective way. To increase the signal-to-noise (S/N) ratio of the GPR data, multi-fold acquisition is performed, and the Common-Mid-Points (CMPs) are acquired. Compared to the traditional CMP method, which is applied to a CMP, the Common-Reflection-Surface (CRS) method is introduced for seismic data processing considering the neighboring CMPs. In addition, instead of a point on the reflector, CRS assumes that the reflector is part of a circle. With these two characteristics, CRS produces a stack section with a high S/N ratio. The Common-Diffraction-Surface (CDS) method, which is a simplified version of CRS, enhances the diffractors related to the underground anomalies like pipeline, flume, and caves. We apply the CDS stack method on a multi-fold GPR data and compare it to the CRS results. These results show that the CDS method can provide a high S/N ratio stack section compared to the traditional CMP method.

1. Introduction

Unlike the Common-Mid-Point (CMP) method, which assumes the horizontal underground reflector Dip-Move-Out (DMO) methods [1], which consider all dipping reflectors, the Common-Reflector-Surface (CRS) stack method is a generalized seismic data-processing that does not consider a point on a reflector but a part of a circle tangent to the reflector [2]. The CRS stack method is based on two hypothetical wave fronts so-called kinematic wave field attribute [3]. Based on these attributes, the second-order approximation of travel time has been developed. The travel time of the CRS operator is obtained by the paraxial ray theory [4, 5] or optic principle [6]. The CRS stack method in a full automatic manner was applied to a seismic data with very promising results [7, 8]. Afterwards an extension was added to the CRS method to handle the conflicting dip [9]. By merging the concept of DMO and CRS methods, the Common-Diffraction-Surface (CDS) stack method was introduced in a data-driven manner so-called data-driven CDS [10-12]. The data-driven CDS method is computationally very expensive, and hence, the model-based CDS stack method has been introduced [13, 14]. The model-based CDS method, which requires a velocity model with a minor accuracy, has been applied successfully to the synthetic and real seismic datasets [15]. The CDS operator enhances the diffractor and can image the reflectors with a reasonable aperture. As the geometry of the multi-fold GPR data is the same as the seismic data acquisition in 2D, and hence, it is possible to processes such a dataset by a seismic processing method like the CRS staking method [16]. Here, we applied the CDS stack method to a multi-fold GPR dataset, which was acquired for environmental studies for water content

Corresponding author: h.shahsavani@uok.ac.ir (H. Shahsavani).

evaluation in SW of Brazil. Then we compared the results obtained with the CRS stack sections.

2. Theory

The CRS stack method is based on two hypothetical wave front experiments: one is related to an exploding point on the reflector so-called Normal-Incident-Point (NIP), which generates a NIP wave with the radius of R_{NIP} at the surface, and the second relates to an exploding surface on the reflector so-called normal wave, which generates an N wave with the radius of R_N at the surface (see Figure 1).

The emergence angle of these two waves is equal to alpha at the surface [3]. Based on these three parameters so-called kinematic wave field attributes, the hyperbolic approximation of travel time reads as:

$$t_{hyp}{}^2 = \left(t_0 + \frac{2\sin\alpha}{v_0}(x_m - x_0) \right)^2 + \frac{2t_0\cos^2\alpha}{v_0}\left(\frac{(x_m - x_0)^2}{R_N} - \frac{h}{R_{NIP}} \right) \quad (1)$$

In this equation, α, R_{NIP}, and R_N are the kinematic wave field attributes, v_0 is the surface wave velocity, $x_m - x_0$ is the relative mid-point, and h is the half offset. The kinematic wave field attributes have to be calculated using the coherence analysis in multi-coverage dataset [18]. As the curvature of a point source is infinite for an underground diffractor, the radius R_N becomes equal to R_{NIP} at the surface for such a diffractor so-called R_{CDS}. Consequently, Equation (1) is simplified to:

$$t_{hyp}{}^2 = \left(t_0 + \frac{2\sin\alpha}{v_0}(x_m - x_0) \right)^2 + \frac{2t_0\cos^2\alpha}{v_0 R_{CDS}}\left((x_m - x_0)^2 - h \right) \quad (2)$$

This equation can image the diffractor in to a full extent, and for the reflector in a reasonable aperture gives acceptable results. The unknown parameters in Equation (2) are α and R_{CDS}. Using the kinematic and dynamic ray tracings, it is possible to obtain R_{CDS} for an arbitrary emergence angle α in a velocity model with a minor accuracy [14]. For more details.

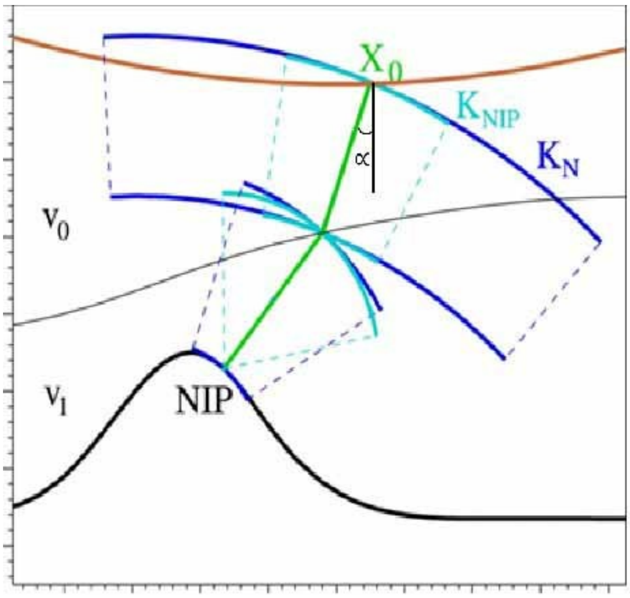

Figure 1. Two hypothetical wave fronts, one related to an exploding surface shown in blue that generates a wave front with a radius of $R_N = 1/K_N$ so-called the Normal (N) wave, and one related to an exploding point that generates a wave front with a radius of $R_{NIP} = 1/K_{NIP}$ at the surface so-called the Normal Incident Point (NIP) wave. Both waves emerge from the surface with the angel α [17].

3. Implementation

The seismic method is based on the measurements of the time that takes a mechanical wave that goes from the source to the receiver. The GPR method is basically the same. However, the GPR method deals with the electromagnetic wave instead of the mechanical wave. Hence, the total acquisition time and the sampling rate in the GPR data are in the order of nanoseconds. In addition, in a common survey for GPR data, the distance between the source and the receiver (offset) is constant along the profile, so called common offset array. By repeating the common offset array along a profile with a different constant offset, the multi-fold GPR dataset is obtained. The multi-fold GPR dataset is geometrically the same as the seismic 2D data set, i.e. time-CMP-offset. Consequently, it is possible to apply the new imaging methods like Common-Reflection-Surface (CRS) [7] or Common-Diffraction-Surface [12, 15] on such datasets, which have not been applied to the GPR dataset till now. In this work, we used the multi-fold GPR data, which acquired a Mala Geophysics Ramac-2 with 200-MHz antenna along a 55 m profile. The multi-fold GPR dataset is uncommon as it is acquired in one channel with a specific offset [16]. The specification of GPR acquisition is presented in Table 1.

The CRS stack method is applied to the multi-fold GPR data. The parameter that was used for the stacking process is shown in Table 2.

We applied the model-based CDS stack to this dataset with the parameters mentioned in Table 3 on a constant velocity model Vconst = 2800 m/s.

The stacked sections of CRS and CDS are shown in Figures 2 and 3, respectively.

Table1. Data acquisition parameters.

Title	Amount
Shot interval	0.1 m
Group interval	0.2 m
Number of shots	546
Number of active channels	28
Number of total trace	33840
Number of CMPs	680
CMP distance	25 m
Sampling interval	1 ns
Number of sample per trace	200
Number of total trace	15302
Number of CMPs	548
CMP distance	25 m
First shot coordinate	(x= 130 cm, y= 0, z= 0)
Last shot coordinate	(x= 5860 cm, y= 0, z= 0)
First geophone coordinate	(x= -190 cm, y= 0, z= 0)
Last geophone coordinate	(x= 5530 cm, y= 0, z= 0)

Table 2. Parameters used for CRS stacking.

Parameter	Amount	Unit
Surface velocity	6000	cm/µs
Mean frequency	200	MHz
Minimum stacking velocity	5500	cm/µs
Maximum stacking velocity	9500	cm/µs
Minimum time	0.015	s
Maximum time	0.08	s
Minimum offset aperture	60	cm
Maximum offset aperture	600	cm
Minimum CMP aperture	100	cm
Maximum CMP aperture	20000	cm

Table 3. Parameters used for CDS stacking.

Parameter	Amount	Unit
Surface velocity	6000	cm/µs
Mean Frequency	200	MHz
Minimum time	0.0	s
Maximum Time	0.08	s
Minimum offset aperture	60	cm
Maximum offset aperture	600	cm
Minimum CMP aperture	100	cm
Maximum CMP aperture	100	cm
Range of Emergence angle	±40	degree
Allow turning rays	No	-

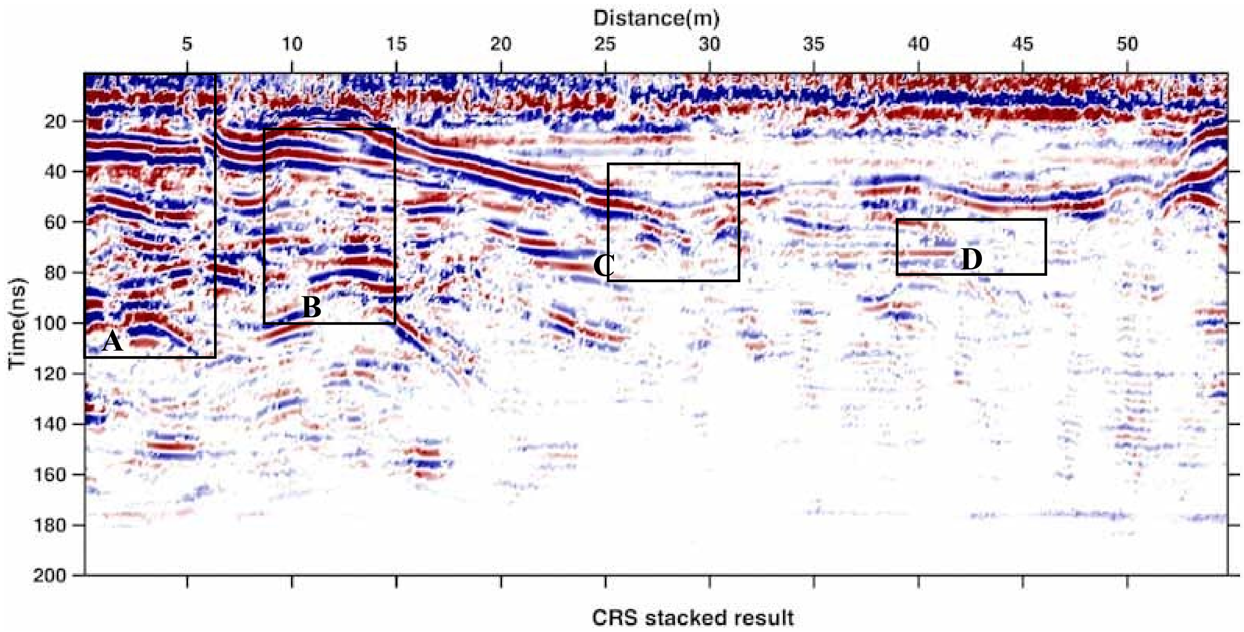

Figure 2. The stacked section with CRS method.

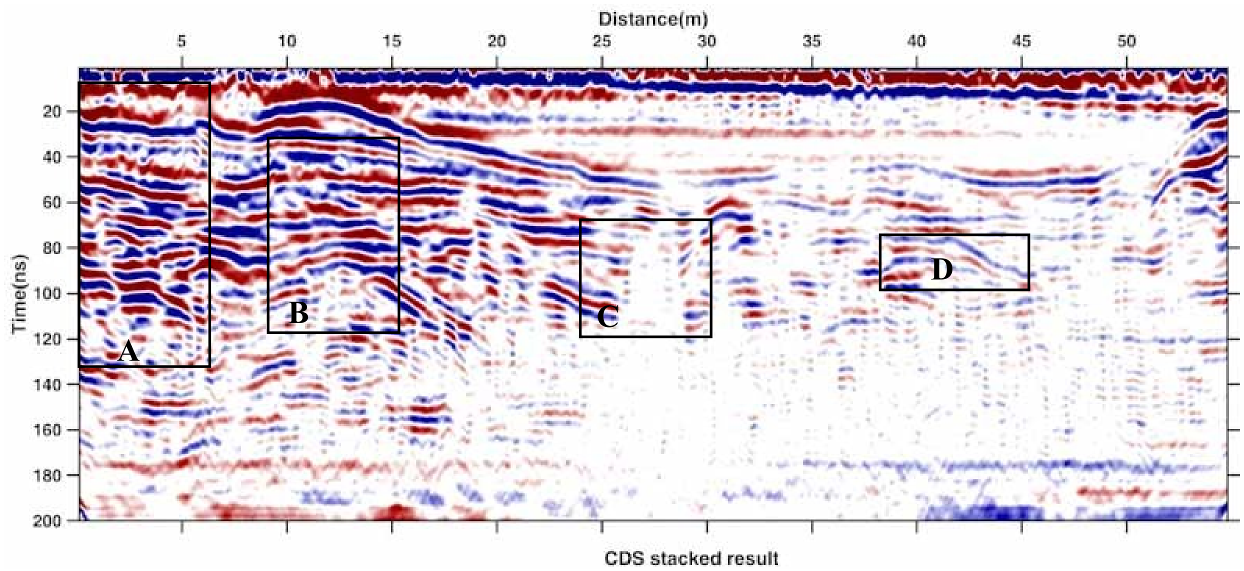

Figure 3. The stacked section with model-based CDS stack method using a constant velocity model V_{const} = 2800 m/s.

The continuity of the reflectors is preserved in the CDS stack section in Figure 3 compared to the CRS stack section shown in Figure 2. For instance, compare the reflector at time 50 ns and distance 7.5 m in Figures 2 and 3. In addition, the fractured points are well-imaged in CDS stacked section, while in the CRS stacked section, such fractions are missing. For example, compare the fraction at time 30 ns and distance 6 m in these two figures.

To have a better comparison, the two stack sections are compared. Figure 4 shows the windows 'A' to 'D' of the two stacked sections depicted in Figures 2 and 3.

As depicted in Figure 4a, processed by the CRS stack method, the continuity of the event is missing from times 20 µs to 110 µs and distance 2.5 m, while the counterpart stacked section, Figure 4b, processed by the CDS stack method, imaged this discontinuity very well. In Figure 4c, after the distance 11.7 m almost for all times, there are just the artifices, while in Figure 4d, all events are well-imaged. In addition, the discontinuities at 67 ns to 92 s at the distances 11.7 m and 14.8 m are clearly imaged. In Figure 4f, it is easy to follow the discontinuity at 58 µs to 83 µs in distance 29.7 m, while this is not clear in Figure 4e. Finally, the events in Figure 4g are like artifices, although these events are smooth and continuous in Figure 4h. The CMP stack section of these datasets is depicted in Figure 5. With the comparison of this figure with the results of CRS and CDS staked section, illustrated in Figures 2 and 3, respectively, it is clearly obvious that the CMP stack method is very inefficient to image many of the events on stacked section.

Finally, comparisons between the frequency contents of the stacked section simulated by the CMP, CRS, and CDS stake methods have been shown in Figures 6a, 6b, and 6c, respectively. The frequency content of the CMP stack section is contaminated by noise of high frequency from 17000 MHz to 30000 MHz. This high frequency disappears in CRS and CDS as these methods use the operator that consider a more number of traces. In addition, the high frequency events in Figure 6 with the frequency around 17000 MHz appear in all sections, which show that the CDS stacked section does not lost the high frequency events.

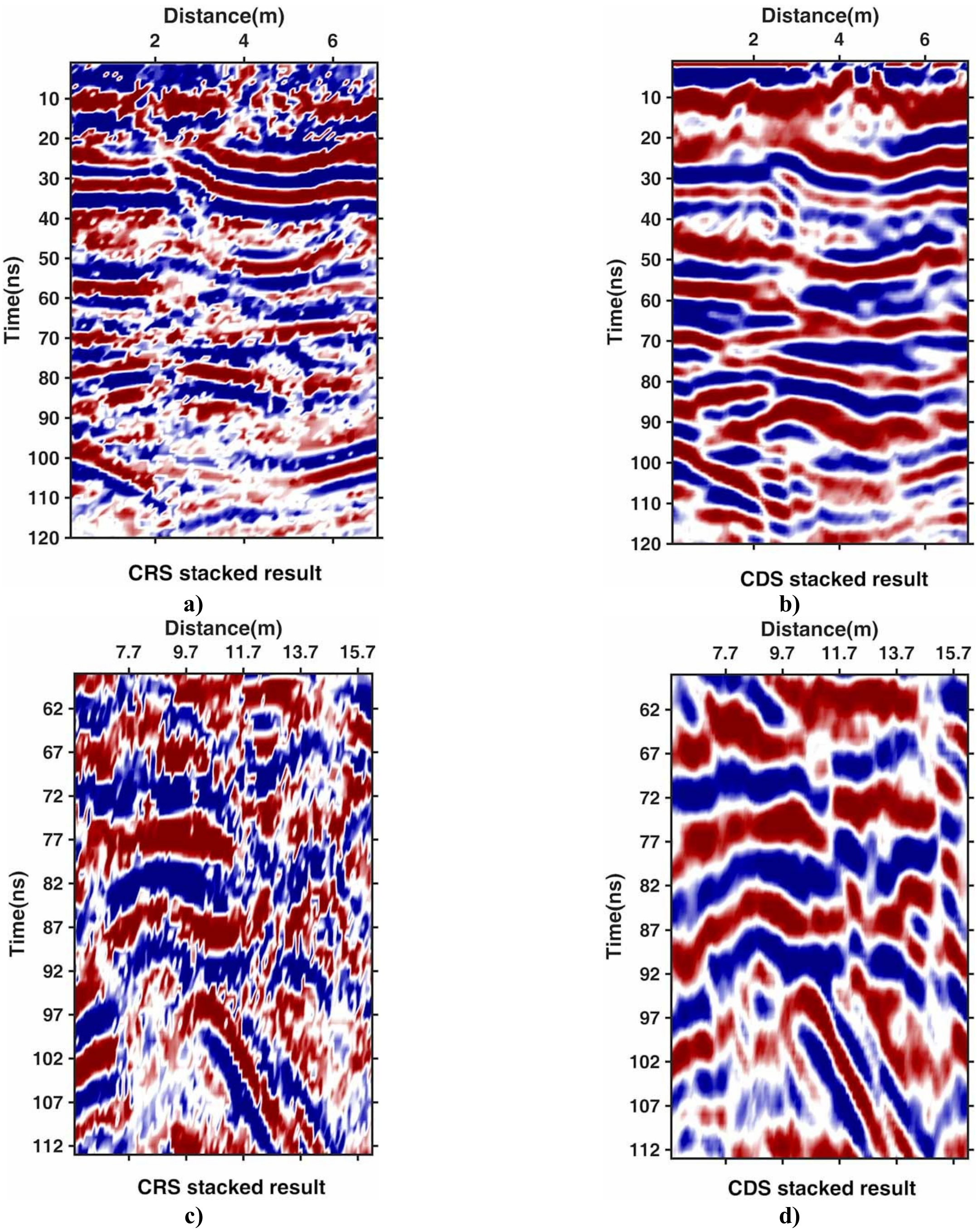

Figure 4. Comparison of four windows of Figures 2 and 3: a- Window ‘A’ in Figure 2, b- Window ‘A’ in Figure 3, c- Window ‘B’ in Figure 2, d- Window ‘B’ in Figure 3, e-Window ‘C’ in Figure 2, f- Window ‘C’ in Figure 3, g- Window ‘D’ in Figure 2, h- Window ‘D’ in Figure 3.

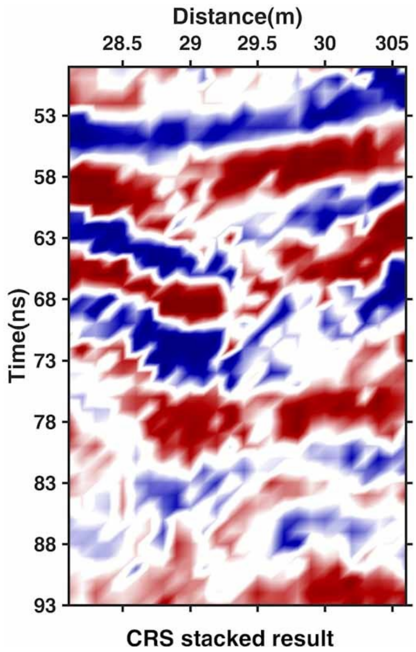

e)

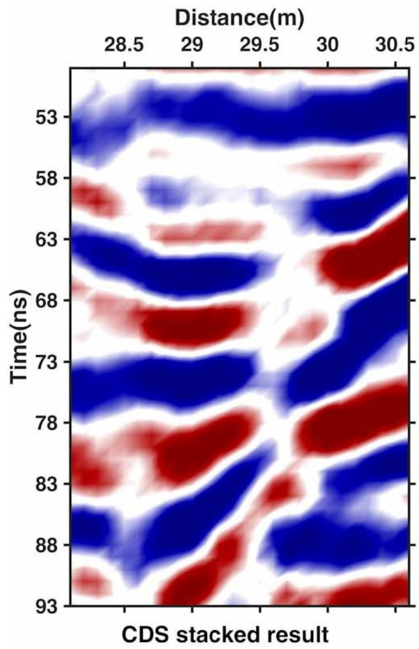

f)

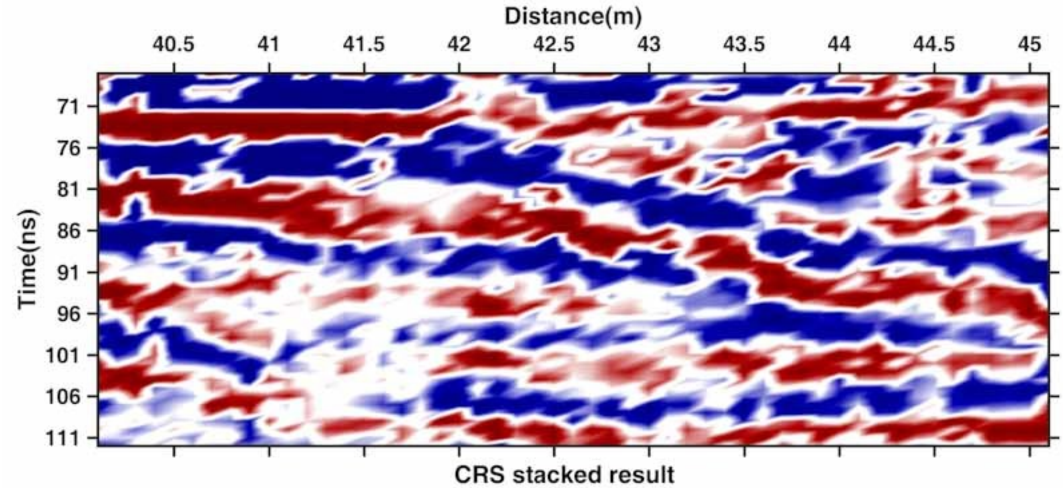

g)

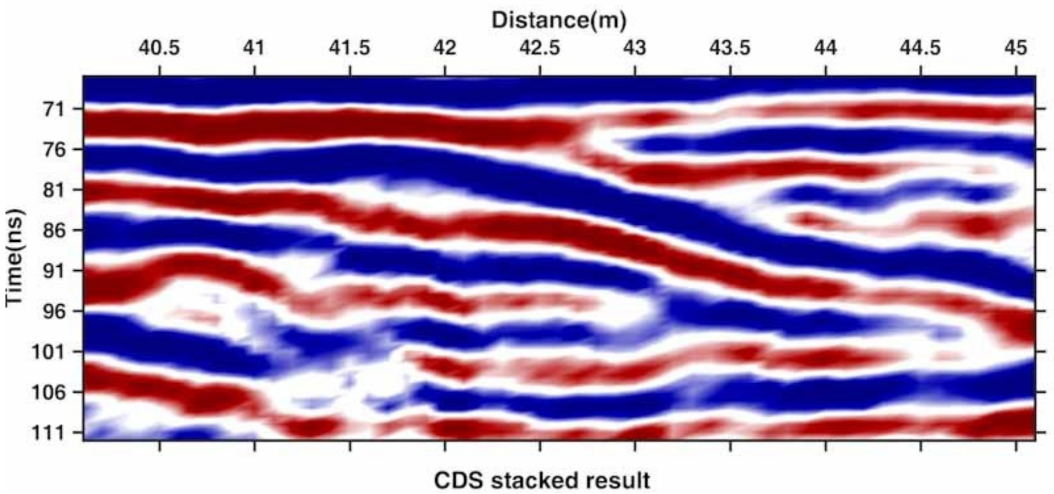

h)

Figure 4. Continued.

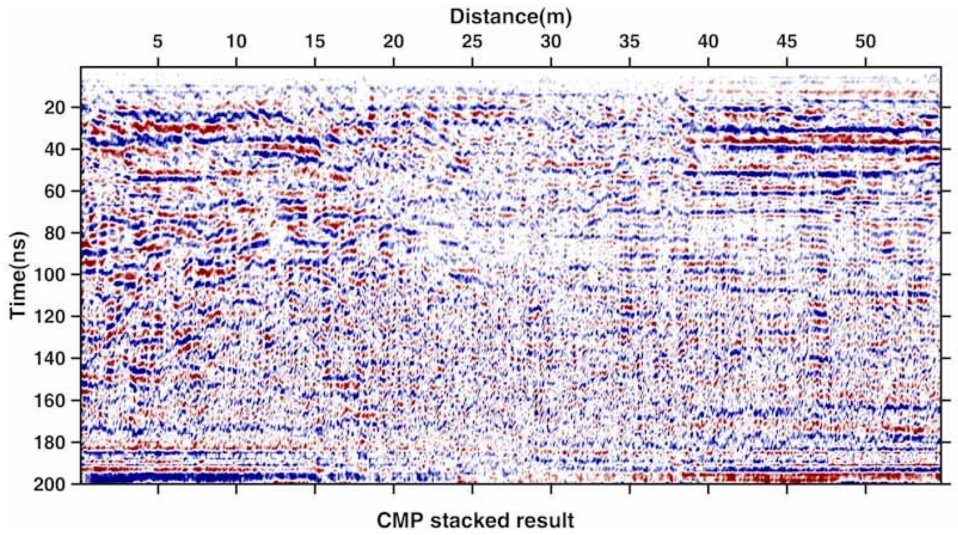

Figure 5. The stacked section with CMP method.

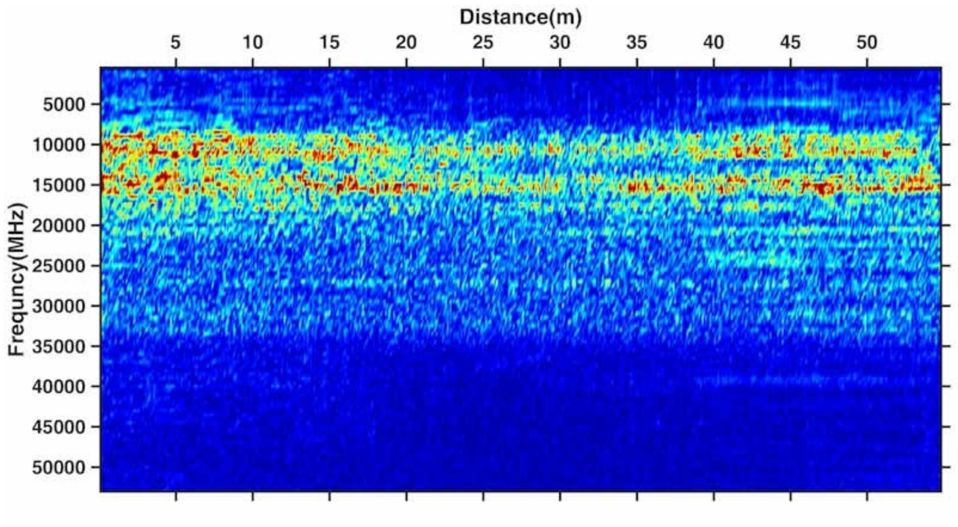

a)

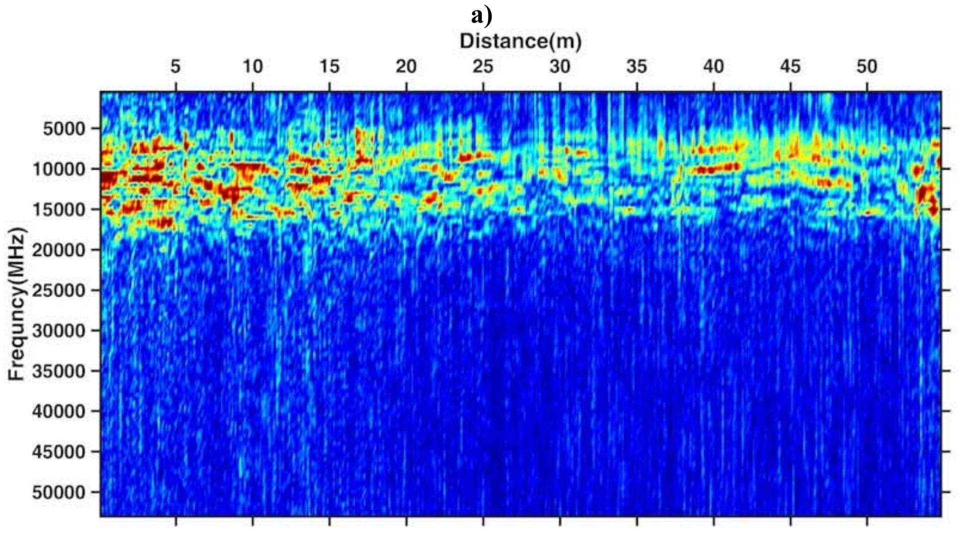

b)

Figure 6. The frequency content of the stacked sections: a) frequency content of the CMP stacked section, b) frequency content of the CRS stacked section, c) frequency content of the CDS stacked section.

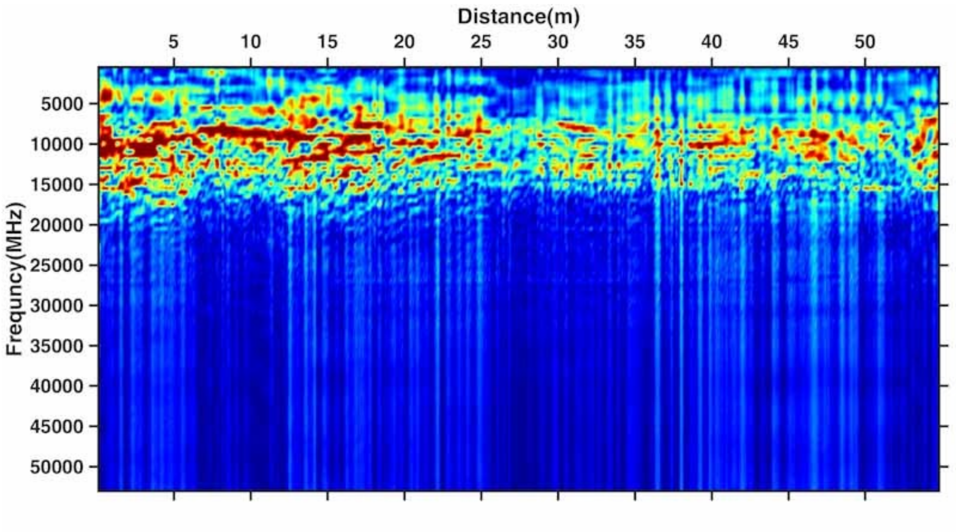

c)
Figure 6. Continued.

4. Conclusions

The Common-Diffraction-Surface stack method, which is a simplification of Common-Diffraction-Surface stack, can simulate the Zero-Offset stack section with a high signal-to-noise ratio. In this work, we applied the CRS and CDS stack methods to multi-fold Ground Penetration Radar (GPR), which is not a common survey. The results obtained show that the stacked CDS sections of the continuity of the events are more preserve than the stacked CRS section. In addition, CDS can image the small fractions very well, while such fractions are missing in the CRS and CMP stacked sections. The frequency contents of the stacked sections for CRS and CDS are almost the same, which shows that the CDS method preserves the high frequency events.

References

[1]. Hale, D. (1984). Dip-moveout by Fourier transform. Geophysics. 49 (6): 741-757.

[2]. Mann, J., Jäger, R., Müller, T., Höcht, G. and Hubral, P. (1999). Common-reflection-surface stack- A real data example. Journal of applied geophysics. 42 (3-4): 301-318.

[3]. Hubral, P. (1983). Computing true amplitude reflections in a laterally inhomogeneous earth. Geophysics. 48 (8): 1051-1062.

[4]. Schleicher, J., Tygel, M. and Hubral, P. (1993). Parabolic and hyperbolic paraxial two-point traveltimes in 3D media. Geophysical Prospecting. 41 (4): 495-513.

[5]. Tygel, M., Müiller, T., Hubral, P. and Schleicher, J. (1997). Eigenwave based multiparameter traveltime expansions. In SEG Technical Program Expanded Abstracts 1997 (pp. 1770-1773). Society of Exploration Geophysicists.

[6]. Höcht, G., De Bazelaire, E., Majer, P. and Hubral, P. (1999). Seismics and optics: hyperbolae and curvatures. Journal of Applied Geophysics. 42 (3-4): 261-281.

[7]. Müller, T. (1998, June). Common reflection surface stack versus NMO/stack and NMO/DMO stack. In 60th EAGE Conference and Exhibition.

[8]. Müller, T., Jäger, R. and Höcht, G. (1998). Common reflection surface stacking method- imaging with an unknown velocity model. In SEG Technical Program Expanded Abstracts 1998 (pp. 1764-1767). Society of Exploration Geophysicists.

[9]. Mann, J. (2002). Extensions and applications of the common reflection surface stack method. Logos-Verlag.

[10]. Soleimani, M., Piruz, I., Mann, J. and Hubral, P. (2009). Common-Reflection-Surface stack: accounting for conflicting dip situations by considering all possible dips. Journal of seismic exploration. 18 (3): 271-288.

[11]. Soleimani, M., Piruz, I., Mann, J. and Hubral, P. (2009, May). Solving the problem of conflicting dips in common-reflection-surface (CRS) stack. In Shiraz 2009-1st EAGE International Petroleum Conference and Exhibition.

[12]. Soleimani, M. (2009). Common Diffraction Surface (CDS) stack; A new approach for solving the problem of conflicting dips. Shahrood, Iran: PhD thesis, Shahrood University of Technology.

[13]. Shahsavani, H., Mann, J., Piruz, I. and Hubral, P. (2011). A model-based approach to the common-diffraction-surface stack—theory and synthetic case study. Journal of Seismic Exploration. 20 (3): 289.

[14]. Shahsavani, H., Mann, J., Piruz, I. and Peter, H. (2011). A model-based approach to the Common-

Diffraction- Surface Stack—theory andsynthetic case study. Journal of Seismic Exploration. 20 (3): 289-308.

[15]. H. Shahsavani. (2011). A model-based approach to the common-diffraction-surface stack. Shahrood, Iran: PhD thesis, Shahrood University of Technology.

[16]. Perroud, H. and Tygel, M. (2005). Velocity estimation by the common-reflection-surface (CRS) method: Using ground-penetrating radar data. Geophysics. 70 (6): B43-B52.

[17]. Heilmann, Z. (2002). The common-reflection-surface stack under consideration of the acquisition surface topography and of the near-surface velocity gradient (Doctoral dissertation, Master's thesis, Karlsruhe University. http://www. wit-consortium. de).

[18]. R. Jäger. (1999). The Common-Reflection-Surface stack theory and application. Karlsruhe, Germany: MSc. thesis, Karlsruhe Institute of Technology.

پردازش داده‌های رادار نفوذ زمینی چند پوششه با استفاده از روش برانبارش سطح پراش مشترک

هاشم شاهسونی

بخش مهندسی معدن، دانشکده مهندسی، دانشگاه کردستان، ایران

ارسال ۲۰۱۹/۴/۱۱، پذیرش ۲۰۱۹/۶/۲۴

* نویسنده مسئول مکاتبات: h.shahsavani@uok.ac.ir

چکیده:

امروزه روش‌های غیر مخرب مورد توجه زیاد دانشمندان قرار گرفته است. یکی از این روش‌ها، روش رادار نفوذ زمینی می‌باشد. با استفاده از این روش می‌توان اطلاعات بسیار با ارزشی را از ساختارهای زیرسطحی بدون تخریب محیط‌زیست و با هزینه اندک به دست آورد. به منظور افزایش نسبت سیگنال به نوفه این روش به صورت چند پوششه برداشت می‌شود و سپس آرایش نقطه میانی مشترک از داده‌های برداشت شده استخراج می‌شود. در مقایسه با روش نقطه میانی مشترک که فقط بر روی یک گروه نقطه میانی مشترک پیاده‌سازی می‌شود، روش برانبارش سطح بازتاب مشترک که به منظور پردازش داده‌های لرزه‌ای توسعه داده شده است، چندین گروه نقطه میانی مشترک را در نظر می‌گیرد. علاوه بر این روش برانبارش سطح بازتاب مشترک به جای یک نقطه روی بازتابنده بخشی از دایره را که منطبق بر بازتابنده است، در نظر می‌گیرد. این دو ویژگی باعث شده است تا این روش، مقاطع برانبارش شده با نسبت سیگنال به نوفه بالاتری نسبت به روش‌های پیشین تولید کند. روش برانبارش سطح پراش مشترک که به نوعی ساده شده روش برانبارش سطح بازتاب مشترک می‌باشد، می‌تواند پراش‌های مرتبط با ناهنجاری‌های زیرسطحی مانند خطوط لوله‌ها، قنات‌ها و غارها را برجسته‌تر سازد. در پژوهش حاضر روش برانبارش سطح پراش مشترک بر روی یک داده چند پوششه رادار نفوذ زمینی پیاده‌سازی شده است. این نتایج با خروجی روش سطح بازتاب مشترک و روش معمول نقطه میانی مشترک مقایسه شده‌اند. نتایج نشان می‌دهد روش سطح پراش مشترک می‌تواند مقاطع دور افت صفر با نسبت سیگنال به نوفه بالاتری را نسبت به روش‌های پیشین ایجاد کند.

کلمات کلیدی: رادار نفوذ زمینی، برانبارش سطح بازتاب مشترک، برانبارش سطح پراش مشترک.